

On the effect of emission lines on the $UBVR$ photometry

A. Skopal¹

Astronomical Institute, Slovak Academy of Sciences, 059 60 Tatranská Lomnica, Slovakia

Received 2 March 2007; accepted 9 April 2007²

Abstract

We investigate the effect on the U , B , V , R_C and R_J magnitudes of the removal of emission lines from a spectrum. We determined Δm corrections from the ratio of fluxes with and without emission lines, transmitted from the object through the photometric filter. An exact and a simplified approach for operative use were applied. The effect was demonstrated for classical symbiotic stars, symbiotic novae and the classical nova V1974 Cyg. It was found that about 20-30%, 30-40%, 10% and 26/20% of the observed flux in the U , B , V and R_C/R_J filter, respectively, is radiated in the emission lines of the investigated classical symbiotic stars. The largest effect was found for symbiotic novae (RR Tel and V1016 Cyg) and the classical nova V1974 Cyg at 210 days (in average of 74%, 79%, 56% and 66/60%), because of their very strong emission line spectrum. In all cases the line corrected flux-points fit well the theoretical continuum. The difference between Δm corrections obtained by the accurate calculation and that given by our approximate formula is less than 10%. Deviations up to 30% can be only in the U passband. Examples for practical application are suggested.

Key words: Techniques: photometric — Stars: emission-line — binaries: symbiotics

PACS: 97.30.Eh, 97.30.Qt, 97.80.Gm

1. Introduction

In many astrophysical applications photometric measurements through the standard U , B , V , R filters are used to analyze radiation in the continuum from stellar objects. For example, a diagnostic by the $(U - B, B - V)$ -diagram is frequently applied to compare the observed colour indices to those of the continuum radiation. However, photometric magnitudes represent integrated fluxes that include both the continuum and the line spectrum. Therefore, a correction for lines has to be applied to obtain photometric flux-points of the true continuum.

The effect on the U , B , V magnitudes of the removal of absorption lines from the spectrum was already introduced by Sandage and Eggen (1959). They found that the absorption lines cause *fainter* magnitudes at all wavelengths. On the other hand the presence of emission lines in the spectral region of the photometric passbands leads to *brighter* magnitudes than those of the continuum. However, it is difficult to quantify this effect. A strong variation of the emission spectrum (e.g. due to outbursts and/or orbital motion),

large differences between individual objects and the complex profile of the true continuum of some interacting binaries (e.g. symbiotic stars, classical novae) preclude a simple solution. Therefore this problem has been approached only individually and without giving a concept for a general application. Probably a first more thorough approach was described by Menzies et al. (1982) who corrected their V magnitudes for strong emission lines in the spectrum of AR Pav. Other authors briefly reported just their results on the emission lines effect to evaluate the continuum level in the optical region (e.g. Fernández-Castro et al. , 1995; Tomov et al. , 2003). Recently Skopal (2003) suggested an accurate calculation of Δm corrections for the UBV passbands.

In this paper we aim to quantify the effect of emission lines on the U , B , V , R_C , R_J magnitudes by the exact approach and to derive an approximate formula for an operative use. In Sect. 2 we introduce our method, in Sect. 3 demonstrate the effect on a sample of selected emission-line objects and in Sect. 4 we briefly discuss our results and suggest their practical application.

¹ E-mail: skopal@ta3.sk

² doi:10.1016/j.newast.2007.04.003

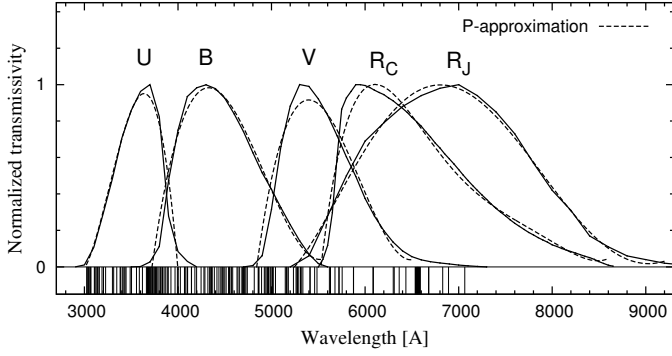


Fig. 1. Response functions for the U , B , V , R_C and R_J filters after Matthews and Sandage (1963), Bessell (1979) and Johnson (1965), respectively. Dashed lines represent their polynomial approximation (Table 1). The bottom band shows distribution of the emission lines from the spectrum of RR Tel (Sect. 3.3.2).

2. The method

2.1. An exact approach

The aim of this paper requires the ratio of the continuum with the superposed emission lines to the line-removed continuum at all relevant wavelengths. Therefore, for the purpose of this paper we express the observed flux in the form

$$F_{\text{obs}}(\lambda) = F_{\text{cont}}(\lambda)(1 + \epsilon(\lambda)), \quad (1)$$

where $F_{\text{cont}}(\lambda)$ is the true continuum (i.e. line-removed continuum) and $\epsilon(\lambda)$ represents the emission line spectrum in units of the continuum at the wavelength λ . Then the magnitude difference, Δm , between the observed magnitude, m_{obs} , and that corresponding to the line-removed continuum, m_{cont} , can be expressed as

$$\Delta m = m_{\text{obs}} - m_{\text{cont}} = -2.5 \log \left[\frac{\int_{\lambda} F_{\text{cont}}(\lambda) S(\lambda) (1 + \epsilon(\lambda)) d\lambda}{\int_{\lambda} F_{\text{cont}}(\lambda) S(\lambda) d\lambda} \right], \quad (2)$$

where $S(\lambda)$ are response functions for the given filter (Fig. 1). We approximate the emission spectrum with an ensemble of Gaussian functions, G_i , as

$$\epsilon(\lambda) = \sum_i G_i(\lambda; \lambda_i, I_i, \sigma_i), \quad (3)$$

where λ_i is the wavelength of the i -th line, I_i its maximum in units of the local continuum and σ_i its HWHM. For the purpose of this work we express the Gauss function in the form

$$G_i(\lambda; \lambda_i, I_i, \sigma_i) = I_i \times \exp \left[-\frac{1}{2} \left(\frac{\lambda - \lambda_i}{\sigma_i} \right)^2 \right]. \quad (4)$$

According to Eq. (2) the removal of emission lines from the spectrum gives *fainter* magnitudes at all wavelengths. Exact calculation of Δm corrections according to Eq. (2) is complicated with modeling the true continuum (Sect. 3). Therefore, for the practical use, we suggest an approximate solution.

Table 1

Polynomial approximation of the transmission functions $S(\lambda) \equiv P(\lambda)$ (Fig. 1) and the constants C_f (Eq. 7).

$P(\lambda) = a_0 + a_1\lambda + a_2\lambda^2 + a_3\lambda^3 + a_4\lambda^4 + a_5\lambda^5$					
f	a_0	a_1	a_2	a_3	C_f
U	169.89	-0.15959	4.9442E-5	-5.0407E-9	567
B	-127.02	0.08009	-1.6508E-5	1.11763E-9	1017
V	-276.23	0.14212	-2.4120E-5	1.35310E-9	876
R_C	-2425.1	1.65606	-4.50068E-4	6.09087E-8	1452
$a_4 = -4.10712E-12, \quad a_5 = 1.104315E-16$					
R_J	345.733	-0.24638	6.8274e-05	-9.1966e-09	2070
$a_4 = 6.03503e-13, \quad a_5 = -1.54735e-17$					

2.2. A simplified approach

In this section we simplify calculation of Eq. (2) with the following assumptions:

- (i) A constant level of the continuum, $F_{\text{cont}}(\lambda)$, within the photometric passbands.
- (ii) Approximation of the $S(\lambda)$ functions by a polynomial function (Fig. 1, Table 1).
- (iii) The response function $S(\lambda)$ is constant within the line, because emission lines are relatively narrow with respect to the width of the photometric filter.
- (iv) According to the relation (4), we express the flux of the i -th line in the continuum units as

$$F_i = \int_{\lambda} G_i(\lambda; \lambda_i, I_i, \sigma_i) d\lambda = \sqrt{2\pi} I_i \sigma_i. \quad (5)$$

Under these assumptions Eq. (2) can be expressed in the form

$$\Delta m_f = -2.5 \log \left[1 + \frac{\sqrt{2\pi}}{C_f} \sum_i P_f(\lambda_i) I_i \sigma_i \right], \quad (6)$$

where the index f denotes the considered filter and $P_f(\lambda_i)$ is the filter transmissivity at the wavelength λ_i of the i -th line given by the polynomial approximation of the corresponding $S(\lambda)$ function, and

$$C_f = \int_{\lambda} S_f(\lambda) d\lambda. \quad (7)$$

The polynomial coefficients and the constants C_f are in Table 1. Both are determined for wavelengths in Å. According to Eqs. (2) and (6), the Δm corrections depend in great deal on the ratio of the line fluxes to the level of the local continuum and their position λ_i (i.e. $P_f(\lambda_i)$). To derive appropriate Δm corrections the spectrum can be in arbitrary units (Eq. (2)).

2.3. Relative contributions from lines

To determine the flux emitted in lines, F_l , relative to the total observed flux, F_{obs} , throughout the given filter (i.e.

the F_l/F_{obs} ratio), we rewrite Eq. (2) in the form

$$\Delta m = -2.5 \log [F_{\text{obs}}/F_{\text{cont}}]. \quad (8)$$

As $F_{\text{obs}} = F_{\text{cont}} + F_l$, the relative amount of radiation emitted in lines can be expressed as

$$F_l/F_{\text{obs}} = 1 - 10^{0.4 \Delta m}. \quad (9)$$

Table 2 introduces these ratios for investigated objects in percents.

3. Analysis and results

To demonstrate the effect of emission lines on the *UBVR* photometric measurements we selected four groups of objects characterized with similar line spectrum and a complex profile of the continuum. They are:

(i) Classical symbiotic stars that display typical quantities of $F_{\text{cont}}(\lambda)$ and I_l , mainly during their quiescent phases. We present examples of AX Per, AR Pav, AG Peg and Z And.

(ii) Objects with a low level of the continuum resulting in higher values of relative line fluxes. We represent this case by the AX Per spectrum during its 1994 total eclipse.

(iii) Objects with very rich and intense emission line spectrum. Here we selected examples of two symbiotic novae, V1016 Cyg and RR Tel.

(iv) Objects with extremely broad and intense lines that usually develop during nebular phases of classical novae. We give example of the V1974 Cyg nova at 210 days.

Following Eqs. (1) and (2) we need the profile of the continuum and the emission line spectrum. We reconstructed the true continuum, $F_{\text{cont}}(\lambda)$, according to Skopal (2005) (hereafter S05). This allow us to compare directly the line-corrected *UBVR* flux-points with the theoretical continuum (Figs. 2, 4–6 below). The emission line spectrum, $\epsilon(\lambda)$, was reconstructed according to relations (3), (4) and (5) with the aid of its parameters available in the literature (mostly fluxes, see below). The *U*, *B*, *V*, *R* magnitudes were converted to fluxes according to the calibration of Henden and Kaitchuck (1982) and Bessell (1979). Simultaneous observations are required, because of a strong variation in the line spectrum and the continuum, mainly in the case of interacting binaries. All observations were dereddened for interstellar extinction. E_{B-V} quantities were taken in most cases from Table 1 of S05.

In the following sections we introduce above mentioned examples. Resulting Δm corrections due to emission lines are listed in Table 2.

3.1. Classical symbiotic stars

3.1.1. AX Per

AX Per is the symbiotic binary with a high orbital inclination. During active phases its light curve shows narrow minima – eclipses – that change into pronounced wave-like

orbitally-related variation during quiescence (e.g. Skopal et al. , 2001).

As the true continuum $F_{\text{cont}}(\lambda)$ we adopted the model of S05 made for ultraviolet observations from 07/11/93 ($\varphi = 0.57$) taken during the post-outburst activity. Figure 2 (a) shows a detail covering the near-UV/optical region. To reconstruct the function $\epsilon(\lambda)$ we used emission lines published by Swings and Struve (1940) and Mao-Lin and Bloch (1954, 1957) observed on 1952 October and 1956 August ($\varphi = 0.5 - 0.6$). They were obtained at the same orbital phase and the level of the activity as those on 07/11/93 (cf. Figs. 2 and 3 of Skopal et al. , 2001). The line intensities were re-scaled with respect to the local continuum according to corresponding intensity tracings presented in the figures of the above referred papers. Quantities of σ_i were adopted to $1-2 \text{ \AA}$ for hydrogen lines and $0.5-1 \text{ \AA}$ for other lines. The *U*, *B*, *V* measurements were taken simultaneously to the IUE spectra (Skopal et al. , 2001). The available magnitude $R_J = 9.83$ was measured on JD 2 446 332 (23/09/85, $\varphi = 0.2$) (Munari et al. , 1992).

The removal of emission lines makes the star’s brightness fainter by 0.43, 0.42, 0.10, 0.17 and 0.11 mag in the *U*, *B*, *V*, R_C and R_J filter, respectively. The corrected *UBVR_J* measurements are close to the predicted continuum (Fig. 2 a).

3.1.2. AR Pav

AR Pav is another eclipsing symbiotic star. The permanent presence of deep and narrow minima in its historical light curve, strong out-of-eclipse variations (e.g. Bruch et al. , 1994) and the observed symbiotic phenomenon, suggest that AR Pav persists in an active phase (S05).

We used the IUE spectra SWP02236 and LWR02023 exposed on 09/08/78 ($\varphi = 0.71$) to model the true continuum (Fig. 2 b). It is very similar to that from 10/05/81 (S05). The line spectrum of AR Pav was reconstructed in part on the basis of observations published by Thackeray and Hutchings (1974), who presented parameters of the strongest emission lines. We note that during active phases of symbiotic stars, profiles of H I and He II emission lines are significantly broader than during quiescence (e.g. Thackeray and Hutchings , 1974; Skopal , 2006). In addition, the function $\epsilon(\lambda)$ was complemented with that for AX Per, because their UV spectra are very similar (Fig. 3). There is no simultaneous photometric measurements to the spectroscopic observations. Therefore we used average *U*, *B*, *V* magnitudes from Andrews (1974) and scaled them so to fit the end of the LWR spectrum. The magnitude $R_C = 10.1$ was taken from Menzies et al. (1982) obtained through their red channel and out of the eclipse.

Also here the largest effect is in the *B* band (-0.55 mag) and smallest in *V* (-0.13 mag). The same value of $\Delta V = -0.13$ mag was derived also by Menzies et al. (1982). The line corrected fluxes fit well the theoretical continuum (Fig. 3 b).

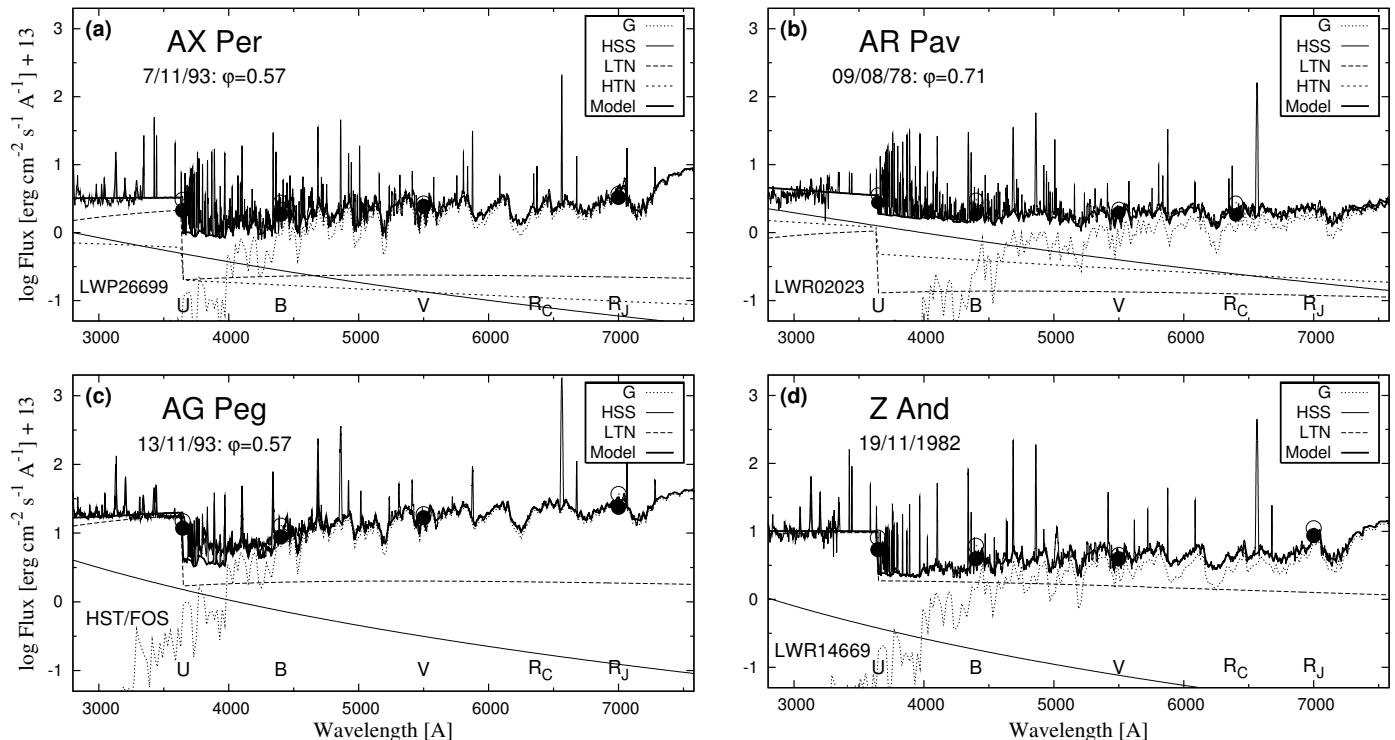


Fig. 2. Reconstructed SEDs for the investigated classical symbiotic stars in the near-UV/optical region. Individual components of radiation are denoted as in S05: HSS (hot stellar source), LTN (low-temperature nebula), HTN (high-temperature nebula) and G (radiation from the red giant). The model (solid thick line = $F_{\text{cont}}(\lambda)$ in Eq. (2)) is given by their superposition. Emission line spectrum, $\epsilon(\lambda)$ (Eq. 3), is superposed on the model. Open and full circles are flux-points of the observed and corrected U , B , V , R_C , R_J magnitudes, respectively.

3.1.3. *AG Peg*

AG Peg is known as the slowest symbiotic nova with eruption in the mid-1850's. Currently it displays all signatures of a classical symbiotic star. Lines of H I and He I vary as a function of the orbital phase with a trend following a slow fading of the star's brightness (Kenyon et al., 1993). In this case it is important to analyze observations taken at the same orbital phase during the same or neighbouring cycles.

As the true continuum we adopted the model made by S05 on the basis of the HST/FOS observations from 13/11/93 ($\varphi = 0.6$, i.e. around the light maximum). Figure 2(c) shows its near-UV/optical part. The function $\epsilon(\lambda)$ was reconstructed according to the line spectrum of the FOS observations to 4780 Å. From this wavelength to 7300 Å we used the line fluxes from the maxima in Table 6 of Kenyon et al. (1993). Quantities of I_i and σ_i were obtained from the fluxes and the level of the local continuum according to their Fig. 1 to satisfy Eq. (5).

The U , B , V measurements were taken from the maximum around JD 2 450 000 according to observations of Tomov and Tomova (1998). The adopted magnitude $R_J = 6.92$ was measured around the 1973 maximum (Ferne, 1985).

For *AG Peg* the true continuum is fainter by 0.19, 0.41, 0.12, 0.40 and 0.31 mag than the star's brightness measured directly through the U , B , V , R_C and R_J filters, respectively. Figure 2(c) shows that the corrected fluxes are close to the predicted continuum. In spite of a relatively high level of the red continuum, the influence of lines to the R -

continuum is significant, because of a strong $H\alpha$ emission.

3.1.4. *Z And*

Z And is a prototype of the class of symbiotic stars. Its historical light curve (from 1887) shows phases of activity with up to 2-3 mag increase of the star's brightness, alternating with periods of quiescence. The quiescent phase is characterized by a complex wave-like light variation as a function of the orbital phase (e.g. Formiggini and Leibowitz, 1994).

As an example of the true continuum we adopted the model of S05 made for 19/11/82 ($\varphi = 0.49$). Figure 2(d) shows its near-UV/optical portion. The line spectrum was reconstructed according to observations published by Fernández-Castro et al. (1995). The relevant spectrum was obtained on 1986 July 12-13. Some weaker lines were added from Mikolajewska and Kenyon (1996) taken on 18/10/86. In addition, the region of the higher members of Balmer lines was enriched with lines from the $\epsilon(\lambda)$ function of *AX Per*. Simultaneous U , B , V measurements were taken from Belyakina (1992). The magnitude $R_J = 8.69$ was estimated from Belyakina's Fig. 1. It corresponds to a maximum during quiescence.

To get the level of the continuum in the U , B , V , R_C and R_J passbands one has to add 0.30, 0.48, 0.12, 0.39 and 0.27 mag, respectively, to the observed values. The corrected fluxes are close to the predicted continuum.

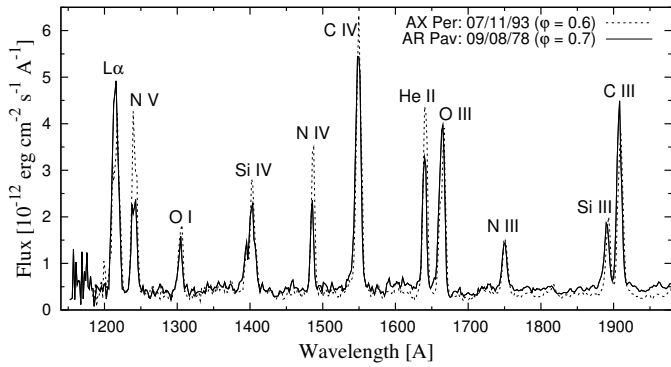


Fig. 3. Close similarity of the ultraviolet spectra of AX Per (07/11/93) and AR Pav (09/08/78). The spectra are dereddened.

3.2. Symbiotic binaries during eclipses

Here we present example of AX Per during its 1994 eclipse, for which ultraviolet and optical spectra as well as photometric observations were available.

The low-resolution spectra from the IUE archive (SWP52027 + LWP29094) taken on 04/09/94 ($\varphi = 0.01$) were used to model the true continuum. It is as faint as $\sim 5 - 6 \times 10^{-14} \text{ erg cm}^{-2} \text{ s}^{-1} \text{ \AA}^{-1}$ and flat in the profile ($T_e(\text{HTN}) \sim 32000 \text{ K}$) in the UV with a dominant contribution from the giant at longer wavelengths beyond the U passband (Fig. 4). The emission line spectrum was taken from Table 4 of Mikolajewska and Kenyon (1992) (observations at eclipses on JD 2447493 and/or JD 2444901) and Table 3 of Skopal et al. (2001) (observation on 05/09/92, $\varphi = 0.01$). A few lines were included from the near-UV of the LWP29094 spectrum. UBV photometric measurements were taken simultaneously to the IUE observations (Skopal et al. , 2001).

The low level of the continuum produces high values of the relative line fluxes (Eq. (5)). As a result the observed photometric flux-points are well above the predicted continuum. The corrected B and V magnitudes fit the continuum well. However, the calculated correction $\Delta U = 0.77 \text{ mag}$ is not sufficient. A correction of $\Delta U \sim 1 \text{ mag}$ is required. This discrepancy is probably caused by incomplete line spectrum within the U passband we had available. Note that in the case of a low level of the continuum also faint emission lines can make a distinctive effect.

3.3. Symbiotic novae

3.3.1. V1016 Cyg

V1016 Cyg underwent its nova-like outburst in 1964 when increased its brightness in the photographic region by about 5 mag, from around 16 to a maximum of ~ 10.5 in 1971. Afterwards it has continued a very slow gradual decrease by less than 1 mag to date (Parimucha et al. , 2000, and references therein). The binary contains a Mira variable as the cool component with a strong IR dust emission observed at/beyond the K band (e.g. Taranova and

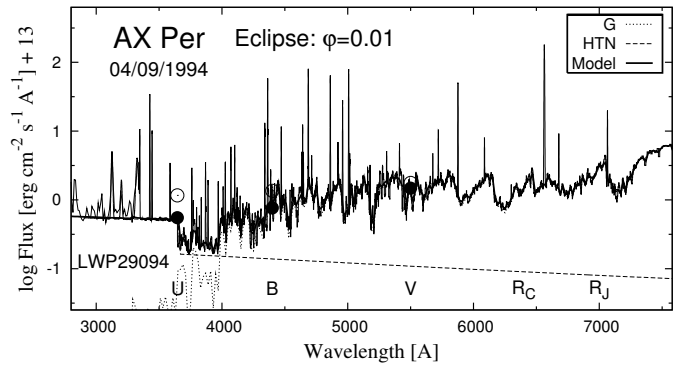


Fig. 4. As in Fig. 2, but for AX Per during its total 1994-eclipse.

Shenavrin , 2000).

We modeled the optical continuum of V1016 Cyg using the IUE spectra SWP24655 and LWP04959 taken on 10/12/84 and the synthetic spectrum for the red giant with $T_{\text{eff}} = 2700 \text{ K}$ and $\log(g) = 0.5$ (Hauschildt et al. , 1999) scaled to the J -band flux, which is assumed to be free of the dust emission (Fig. 5 a). The line spectrum was reconstructed from emission line fluxes published by Schmid and Schild (1990). The spectrum was taken on 15/11/87 at the INT telescope. The $UBVR_J$ and J photometry was taken from Munari et al. (1992), Parimucha et al. (2000) and Taranova and Shenavrin (2000). Observations were dereddened with $E_{B-V} = 0.28$ (Schmid and Schild , 1990).

We found that the removal of emission lines makes the star's brightness fainter by 1.23, 1.67, 1.19, 1.87 and 1.57 mag in the U , B , V , R_C and R_J band, respectively. The corrected photometric fluxes fit perfectly the model continuum.

3.3.2. RR Tel

RR Tel underwent a nova-like outburst in 1944 (Penston et al. , 1983). The light curve shows a gradual fading from the maximum with the visual magnitude around 11.4 during 2000-02 (see Fig. 1 of Kotnik-Karuza et al. , 2006). The binary comprises a white dwarf as the hot component and a Mira-type variable as the cool component. Its circumstellar environment produces a strong nebular and dust emission (e.g. Contini and Formigini , 1999).

We determined the true continuum by modeling the HST/STIS spectrum (1140 – 7050 Å) taken on 18/10/2000 with the aid of the IR photometry published by Kotnik-Karuza et al. (2006). The near-UV/optical region is very similar to that of V1016 Cyg (Fig. 5). The emission line spectrum, $\epsilon(\lambda)$, was reconstructed from the observed line fluxes and the level of the local continuum. We used the $UBVR_C$ magnitudes according to Munari et al. (1992). They were obtained in 1990.5, i.e. about 10 years prior to the HST observation (2000.8), when the star was brighter by $\sim 0.7 \text{ mag}$ in the visual region (see Fig. 1 of Kotnik-Karuza et al. , 2006). Observations were dereddened for interstellar extinction with $E_{B-V} = 0.10$ (Young et al. , 2005).

Table 2

Corrections $\Delta m(2)$ and $\Delta m(6)$ of the $UBVR_C R_J$ photometry for emission lines calculated according to Eqs. (2) and (6), respectively. The relative amount of radiation emitted in lines and transmitted through the given filter (i.e. the F_l/F_{obs} ratio in Eq. (9)) is in percents.

Object	$\Delta U(2)/\Delta U(6)$		$\Delta B(2)/\Delta B(6)$		$\Delta V(2)/\Delta V(6)$		$\Delta R_C(2)/\Delta R_C(6)$		$\Delta R_J(2)/\Delta R_J(6)$	
	[mag]	[%]	[mag]	[%]	[mag]	[%]	[mag]	[%]	[mag]	[%]
AG Peg	-0.19/-0.26	16/21	-0.41/-0.40	31/31	-0.12/-0.13	10/11	-0.40/-0.39	31/30	-0.31/-0.35	25/28
Z And	-0.30/-0.35	24/28	-0.48/-0.48	36/36	-0.12/-0.14	10/12	-0.39/-0.44	30/33	-0.27/-0.38	22/30
AR Pav	-0.40/-0.49	31/36	-0.55/-0.55	40/40	-0.13/-0.15	11/13	-0.37/-0.36	29/28	-0.29/-0.30	23/24
AX Per	-0.43/-0.56	30/40	-0.42/-0.48	32/36	-0.10/-0.12	9/10	-0.17/-0.20	14/17	-0.11/-0.16	10/14
AX Per Ecl.	-0.77/-0.60	51/42	-0.62/-0.64	44/45	-0.19/-0.33	16/26	-0.27/-0.32	22/26	-0.17/-0.26	14/21
RR Tel	-1.71/-1.67	79/78	-1.68/-1.74	79/80	-0.87/-0.97	55/59	-0.98/-1.04	59/62	-0.73/-0.89	49/56
V1016 Cyg	-1.23/-1.15	68/65	-1.67/-1.71	78/79	-1.19/-1.33	67/71	-1.87/-1.61	82/77	-1.57/-1.46	76/74
V1974 Cyg	-1.57/-1.51	76/75	-1.73/-1.75	80/80	-0.66/-0.77	46/51	-0.94/-0.94	58/58	-0.88/-0.86	56/55

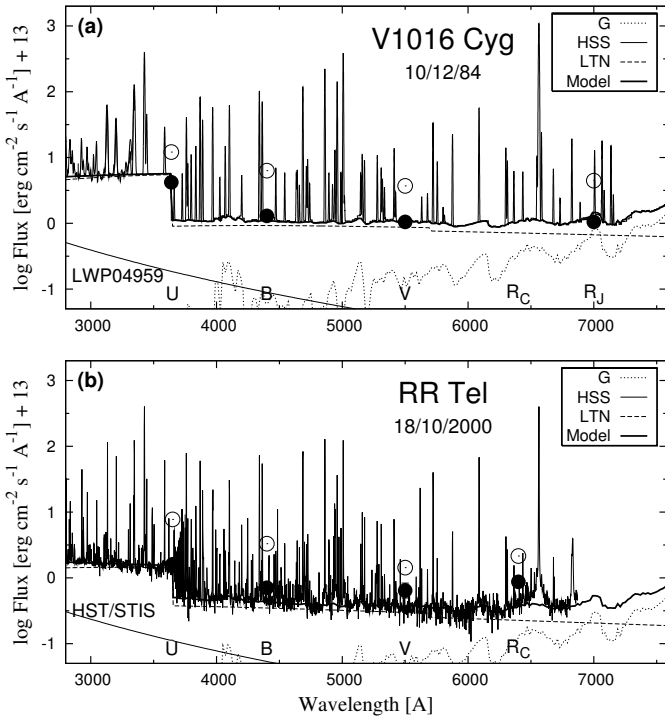


Fig. 5. As in Fig. 2, but for symbiotic novae V1016 Cyg and RR Tel.

The influence of emission lines to the true continuum is significant. We found that RR Tel emitted about 79, 79, 55, 59 and 49% of the observed light in the emission lines throughout the U , B , V , R_C and R_J filter, respectively. However, the flux-points of the line corrected magnitudes are still placed above the true continuum, because the photometric observations were carried out at a higher star's brightness than that corresponding to the HST observations.

3.4. Classical nova V1974 Cyg

The classical nova V1974 Cyg (Nova Cygni 1992) was discovered by Collins (1992) on 1992 February 19. It reached a peak visual magnitude of 4.4 on 1992 February 20.7 UT

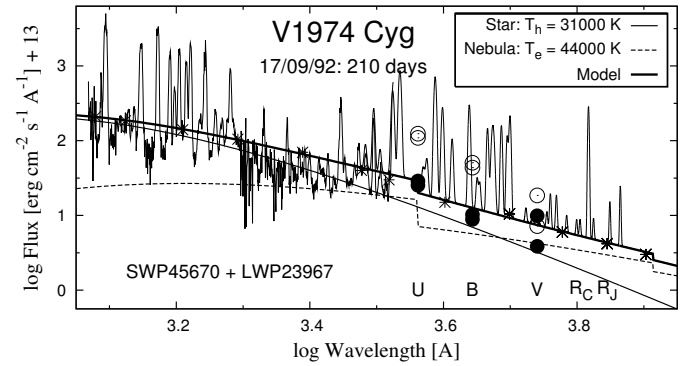


Fig. 6. Spectrum of the classical nova V1974 Cyg during the nebular phase at 210 days. It was composed from ultraviolet IUE and optical spectra of Austin et al. (1996). Continuum fluxes are denoted by (*). The model SED (solid thick line) is described in the text. Different magnitudes were obtained at different observatories.

(Schmeer, 1992). V1974 Cyg developed an emission line spectrum at early stages of its evolution. First nebular lines appeared in 1992 April and in 1992 September dominated the ultraviolet and optical spectrum (Chochol et al., 1993; Austin et al., 1996). To demonstrate the effect of emission lines on the U , B , V measurements we used observations from the nebular phase taken in 1992 September. Observations were dereddened with $E_{B-V} = 0.36$ (Austin et al., 1996).

We reconstructed the continuum using the low-resolution IUE spectra SWP45670 and LWP23967 exposed on 17/09/92 (i.e. 210 days after the maximum) and the optical/near-IR spectra published by Austin et al. (1996). As the latter spectroscopy was not simultaneous with the former one, we interpolated spectra made at 40 and 400 days to 210 days after the maximum. It was possible, because the continuum profile did not change significantly (cf. Figs. 4 and 5 of Austin et al., 1996). Then we scaled fluxes from the near-UV to those of the IUE observations and selected 12 flux-points in the continuum between 1280 and 8000 Å, considering the influence of the iron curtain as proposed by Shore and Aufdenberg (1993). Following to S05 we modeled the continuum fluxes by a two-component-

model including contributions from a star and nebula. In our model SED (Fig. 6) the source of the stellar radiation has an effective radius $\theta_h = 2.4 \pm 0.8 \times 10^{-11}$ and radiates at $T_h = 31\,000 \pm 5\,000$ K, while the nebula radiates at $T_e = 44\,000 \pm 5\,000$ K having the emission measure, $EM = 4\pi d^2 \times (13.8 \pm 3) 10^{15} \text{ cm}^{-3}$. We note that the observed stellar radiation is not capable of giving rise the nebular emission by photoionization, because of too low T_h . This implies that a major part of the nebular radiation is due to collisions, which is consistent with its high electron temperature and the presence of a fast outflow from the nova.

The line spectrum of V1974 Cyg was reconstructed according to observations of Chochol et al. (1993) taken at 212 days (see their Figs. 5 and 6) and Austin et al. (1996) (211 days, Table 7), obtained nearly simultaneously with the ultraviolet observations. The U , B , V measurements obtained on 17/09/92 were taken from Chochol et al. (1993).

For V1974 Cyg the effect of emission lines on the U , B , V and R magnitudes is significant: $\Delta U = 1.57$, $\Delta B = 1.73$, $\Delta V = 0.66$, $\Delta R_C = 0.94$ and $\Delta R_J = 0.88$ mag. Disagreement between the corrected V magnitude and the predicted continuum at 5500 \AA is caused by a large scatter in the V measurements obtained at different observatories at the time of the presence of strong nebular emissions in the V1974 Cyg spectrum (see Fig. 8 of Chochol et al. , 1993). Note that the strongest nebular lines ($\lambda 4959$ and $\lambda 5007$) are placed at the steep edge of the V filter (Fig. 1).

4. Discussion

4.1. Comparison of exact and simplified solution

Deviations between Δm corrections obtained by the accurate calculation (Eq. 2) and by our approximate relation (Eq. 6) are less than 10% for B , V , R_C , R_J measurements (Table 2). A systematic shift for the R_J passband ($\Delta R_J(2) < \Delta R_J(6)$) is due to the slope of the red giant continuum here. This increases the effective wavelength of the R_J filter and thus the contribution from the continuum, which results in a smaller (correct) Δm than that estimated for a constant continuum (cf. Eq. (2)). Larger differences are for ΔU corrections, because of a marked difference between the true and the assumed constant continuum profile around the Balmer discontinuity. To get a satisfactory result in U for objects with a strong Balmer jump in emission, we multiplied the sum in Eq (6) by a factor of 0.8.

4.2. Examples for practical applications

Corrections Δm can be used to convert arbitrary flux units of an emission-line spectrum to fluxes in absolute units with the aid of the simultaneous $UBVR$ photometry. The following steps are relevant.

(i) Appropriate Δm can be estimated according to Eq. (6) to obtain magnitudes of the line-removed continuum.

(ii) To deredden the continuum-magnitudes and convert them to fluxes as referred in Sect. 3.

(iii) A polynomial fit to the line corrected flux-points of the photometric passbands can be adopted as the true continuum.

In special cases it is sufficient to limit this calibration just to one passband to get an appropriate scaling factor. Usually this takes effect for a spectrum exposed within the R band which contains one strongly dominant emission from $H\alpha$ (e.g. symbiotic stars). In this case Eq. (6) can be expressed as

$$\Delta m_\alpha = -2.5 \log[1 + P_R(6563)F_\alpha/C_R], \quad (10)$$

where F_α is the $H\alpha$ flux in units of the local continuum, transmissivities $P_{R_C}(6563) = 0.79$, $P_{R_J}(6563) = 0.92$ and C_R quantities (Eq. (7)) are in Table 1.

A proper corrections for emission lines must be applied to model multicolour light curves of the outbursting objects, spectra of which are very rich for emission lines. For example, Hachisu et al. (2006) restricted their calculation of theoretical light curves of the 2006-outburst of the recurrent symbiotic nova RS Oph only to the y and I_C filters to avoid contamination by the strong emission lines, although B and R_C measurements were also available.

The effect of emission lines on the photometric measurements changes also the colour indices. Generally, Δm corrections are different in different passbands, which results in a relevant change in the colour indices of the true continuum. Therefore, prior to a diagnostic of the emission-line objects by colour diagrams one has to correct the observed indices for the light excess due to the emission lines. This approach can be effectively used to study evolution of the composite spectra of, for example, symbiotic stars on the basis of their multicolour light curves. However, this represents rather sophisticated task and we will devote to this problem in a separate paper.

5. Conclusions

We investigated the effect on the U , B , V and R magnitudes of the removal of the emission lines from the spectra of some classical symbiotic stars, symbiotic novae and the classical nova V1974 Cyg. Our results may be summarized as follows:

(i) We calculated the ratio of fluxes with and without the lines, transmitted through the given photometric filter, to obtain corrections ΔU , ΔB , ΔV , ΔR_C and ΔR_J caused by emission lines. First, we approached this problem by a precise reconstruction of the true continuum (Eq. 2). Second, we derived a formula to estimate these corrections by a simple way for an operative use (Eq. 6). Deviations between Δm corrections determined by both the methods are less than 10%. Larger differences are in the U passband,

because of a complex profile of the true continuum at this region.

(ii) The removal of emission lines makes the star's brightness fainter by $\Delta U \sim 0.33$, $\Delta B \sim 0.46$, $\Delta V \sim 0.12$, $\Delta R_C \sim 0.33$ and $\Delta R_J \sim 0.25$ mag for the selected symbiotic stars (Table 2). The effect is larger for AX Per at the eclipse, because of the low level of the continuum (e.g. $\Delta U = 0.77$ and $\Delta B = 0.62$ mag). The largest corrections were found for the symbiotic novae and the nebular phase of the classical nova V1974 Cyg ($\Delta U \sim 1.5$, $\Delta B \sim 1.7$, $\Delta V \sim 0.91$, $\Delta R_C \sim 1.3$ and $\Delta R_J \sim 1.1$ mag), because of their very intense emission line spectrum. The significant effect in R passbands is mainly due to a strong $H\alpha$ emission and the high transmissivity of both R_C and R_J filters at $\lambda 6563 \text{ \AA}$ (Eq. (10), Table 1, Fig. 1).

(iii) The line corrected $UBVR$ flux-points fit well the modeled continuum (Figs. 2 and 4–6). Thus they can be used in many astrophysical applications for studying the continuum of emission-line objects (Sect. 4.2).

Acknowledgments

This research has been in part supported by the Slovak Academy of Sciences under a grant No. 2/7010/7. The code for calculating Δm corrections according to Eq. (6) is available at <http://www.astro.sk/~astrskop/ubvr.corr/>.

References

Andrews, P.J., 1974. MNRAS 167, 635
Austin, S.J., Wagner, R.M., Starrfield, S., et al., 1996. AJ 111, 869
Belyakina, T.S., 1992. Izv. Kr. Astrophys. Obs. 84, 49
Bessell, M.S., 1979. PASP 91, 589
Bruch, A., Niehues, M., Jones, A.F., 1994. A&A 287, 829
Chochol, D., Hric, L., Urban, Z., et al., 1993. A&A 277, 103
Collins, P., 1992. IAU Circ. No. 5454
Contini, M., Formigini, L., 1999. ApJ 517, 925
Fernández-Castro, T., González-Riestra, R., Cassatella, A., et al., 1995. ApJ 442, 366
Ferne, D.J., 1985. PASP 97, 653
Formigini, L., Leibowitz, E.M., 1994. A&A 292, 534
Hachisu, I., Kato, M., Kiyota, S., et al., 2006. ApJ 651, L141
Hauschildt, P.H., Allard, F., Ferguson, J., et al., 1999. ApJ 525, 871
Henden, A.A., Kaitchuck, R.H., 1982. Astronomical Photometry, Van Nostrand Reinhold Company, New York, 50
Johnson, H.L., 1965. ApJ 141, 923
Kenyon, S.J., Mikolajewska, J., Mikolajewski, M., et al., 1993. AJ 106, 1573
Kotnik-Karuza, D., Friedjung, M., Whitelock P. A., et al., 2006. A&A 452, 503
Mao-Lin, T., Bloch, M., 1954. Ann. d' Astrophys. 17, 6
Mao-Lin, T., Bloch, M., 1957. Ann. d' Astrophys. 20, 86
Matthews, T.A., Sandage, A.R., 1963. ApJ 138, 30

Menzies, J.W., Coulson, I.M., Caldwell, J.R.A., Corben, P.M., 1982. MNRAS 200, 463.
Mikolajewska, J., Kenyon, S.J., 1992. AJ 103, 579
Mikolajewska, J., Kenyon, S.J., 1996. AJ 112, 1659
Munari, U., Yudin, B.F., Taranova, O.G., et al., 1992. A&AS 93, 383
Parimucha, Š, Arhipova, V.P., Chochol, D., et al., 2000. Contrib. Astron. Obs. Skalnaté Pleso 30, 99
Penston, M.V., Benvenuti, P., Cassatella, A., et al., 1983. MNRAS 202, 833
Sandage, A.R., Eggen, O.J., 1959. MNRAS 119, 298
Schmeer, P. 1992, IAU Circ. No. 5455
Schmid, H.M., Schild, H., 1990. MNRAS 246, 84
Shore, S.N., Aufdenberg, J.P., 1993. ApJ 416, 355
Skopal, A., 2003. Baltic Astronomy 12, 604
Skopal, A., 2005. A&A 440, 995 (S05)
Skopal, A., 2006. A&A 457, 1003
Skopal, A., Teodorani, M., Errico, L., et al., 2001. A&A 367, 199
Swings, P., Struve, O., 1940. ApJ 91, 546
Taranova, O.G., Shenavrin, V.I., 2000. Astron. Letters 26, 600
Thackeray, A.D., Hutchings, J.B., 1974. MNRAS 167, 319
Tomov N.A., Tomova, M.T., 1998. IBVS No. 4574
Tomov, N.A., Taranova, O.G., Tomova, M.T., 2003. A&A 401, 669
Young, P.R., Berrington, K.A., Lobel, A., 2005. A&A 432, 665